Weld Cladding with Austenitic Stainless Steel for Imparting Corrosion Resistance

Biswajit Khara[1], Nanda Dulal Mandal[2], Anindya Sarkar[3], Mithun Sarkar[4], Bhaskar Chakrabarti[5] and Santanu Das[6*]

Department of Mechanical Engineering, Kalyani Government Engineering College,
Kalyani- 741 235, West Bengal, India
*Corresponding author : sdas.me@gmail.com

ABSTRACT

Weld cladding is a process of depositing a thick layer of a material on a corrosion-, or erosion-, prone material to protect it from corrosion or erosion respectively. In this process, service life of the clad component increases substantially even under hostile conditions. In the present work, austenitic stainless steel cladding is done on low alloy steel specimens to make the clad components resistant to corrosion wearing under a chemically reactive environment. Corrosion-resistance characteristics of clad layer is explored along with its dependency on clad bead geometry, clad composition, etc. that are controlled by process parameters. It is, therefore, essential to select appropriate process parameters to obtain sound clad quality. Experiments are conducted on cladding with austenitic stainless steel on low alloy steel plates under varying conditions using gas metal arc welding. Performance of cladding is experimentally explored to find out suitable parameter combination to obtain high corrosion resistance. At 100 A weld current, 8.7 mm/s torch travel speed and 24 V weld voltage, minimum corrosion rate is seen, and hence, may be adopted in practice.

Keywords: Cladding, welding, GMAW, MAG, stainless steel, austenitic steel, corrosion resistance.

1.0 INTRODUCTION

Weld cladding is a process of depositing a thick layer of corrosion or erosion resistance material on a base material to reduce rate of corrosion or erosion [1-4]. Cladding is employed to increase service life of engineering components under hostile conditions. Weld cladding technology is being looked into by many researchers, and are now applied in various industries, such as chemical, petrochemical, fertilizer, food processing industries, nuclear and steam power plants, etc. In majority of applications, cladding is employed for imparting resistance to corrosion. In low carbon or low alloy steel components, usually stainless steel is deposited to suppress the rate of corrosion.

Various welding processes were employed [1-12] for cladding or other material deposition methods, such as shielded metal arc welding (SMAW), submerged arc welding, gas tungsten arc welding (GTAW), plasma arc welding (PAW), gas metal arc welding (GMAW), flux cored arc welding (FCAW), electro-slag welding (ESW), oxy-acetylene welding, explosive welding, etc. Composition of clad material, quality of bonding and shape of clad bead influence clad quality. Again, acceptable clad bead geometry depends on various parameters, such as, wire feed rate, welding speed, arc voltage, etc. Hence, development of the relationship between process parameters and bead geometry is necessary to help select of appropriate process parameters.

A number of research works was done to explore dependence of process parameters on clad quality using FCAW [1, 2], GMAW [3, 4, 6], laser and plasma transferred arc (PTA) welding [7], etc. for different clad materials and workpiece combinations. Variety of stainless steels, specially, austenitic stainless steels [7, 8, 10-12] and duplex stainless steels [4-6] were tried for cladding to improve corrosion resistance. Nickel alloys were also attempted [13] for cladding accessories of power plant boiler to impart high temperature corrosion resistance.

Kumar et al. [14] investigated on the variation of dilution under varying process parameters of GMAW during cladding of stainless steel cladding on mild steel, while Ghosh and others [15] carried out experimental works using pulsed current GMAW during stainless steel cladding on structural steel plates, Nouri and others [16] explored effects of cladding condition on dilution and bead geometry. Palani and others [1, 2] and Kannan and others [3, 5] undertook the investigative works on weld cladding with stainless steels under different parametric conditions. Chakrabarti et al. [4] carried out detailed investigation on the performance of flux-cored duplex stainless steel clad structural steel using synergic as well as pulsed mode of GMAW at some heat inputs under different gas shields. In some similar direction, Verma et al. employed austenitic stainless steel [11] and duplex stainless steel [17] electrode to clad low alloy steel to find out the conditions giving low corrosion resistance.

Different corrosion testing techniques were adopted [18-20] to evaluate anti-corrosive properties of clad objects. When acceptable corrosion resistance was achieved, the parameter combine was recommended for cladding. GMAW was observed to show good cladding; however, to have quality cladding using GMAW, appropriate process parameters should be selected. Many investigations were made [21-25] in the past in this direction for optimal selection of process parameters. While some researchers used the Analytic Hierarchy Process (AHP) [21, 25] for this purpose, grey-based Taguchi method [22], genetic algorithm [23], etc. for process parameter selection.

In this work, low alloy steel base plates are clad with 316 austenitic steel electrode using gas metal arc welding (GMAW) applying 100% CO_2 gas shield at different welding current and weld traverse speed to evaluate desirable quality of cladding to offer good resistance to corrosion. To achieve this, first bead-on-plate trial runs are conducted. Following the observations of these experiments, cladding experiments are carried out to evaluate suitable process parameters to obtain good corrosion resistance properties.

2.0 EXPERIMENTAL DETAILS

Main purpose of providing anti-corrosive cladding is to improve corrosion resistance of an engineering component or facility. Cladding on low alloy steel base plate is done in this work by austenitic stainless steel using an ESAB, India made gas metal arc welding machine (model: AutoK400) with 60% duty cycle to find out effects of input parameters on clad quality. 100% CO_2 gas shield is used in all the experiments performed. The base plate selected is of 100 mm × 50 mm × 5 mm size, and has a composition of 0.08% C, 0.18% Si, 0.06% S, 0.07% P, 0.4% Mn, 1.22% Ni, 2.02% Cr and the rest being Fe. Filler wire selected is of austenitic stainless steel (Code 316) with filler wire diameter of 1.2 mm. It is having 0.09% C, 0.32% Si, 0.014% S, 0.033% P, 1.33% Mn, 10.7% Ni, 17.16% Cr, 2% Mo and the rest being Fe.

Trial runs are first conducted following the condition shown in **Table 1.** Trial runs are done as bead-on-plate experiments on the same low alloy steel plates with the same 1.2 mm diameter austenitic stainless steel wire electrode under 100% CO_2 gas shield. Heat input, HI at each experimental run is estimated using a relationship,

$$HI = \eta V I / (1000 S) \quad (1)$$

where, η is efficiency, V is weld voltage, I is weld current and S is welding torch speed. Values of heat input are shown in **Table 1.** Welding current and welding speed are varied, and continuity of weld deposition, spatter and weld geometry parameters are observed. Reinforcement, R and bead width, W are measured under a Mitutoyo, Japan made tool makers' microscope after polishing the specimen cross section. From these, reinforcement form factor (RFF= W/R) is calculated. At quite less heat input, weld beads formed has less continuity. This may be due to low heating and less volume of molten material deposited on the base plate. On the other hand, too high heat input more than 0.50 kJ/mm does not give acceptable bead with moderate to large spatter as a natural phenomenon.

A two-factor three-level (**Table 2**) experiment is designed following full factorial design of experiments for undertaking cladding experiments taking welding current (I) and welding speed (S) as two independent variables. Range of parameters is set in this cladding experiment after observing the results obtained from trial runs. Cladding is done in the following way. First, weld beads are made with zero overlap. Next, the weld bead is deposited in each of the gaps between two successive passes made earlier as detailed in **Fig. 1.** After cladding, clad material hardness, its microstructure and corrosion resistance are observed.

Hardness Testing is done on a Rockwell Hardness Testing machine. For microstructure testing, samples are polished in a belt grinder/polisher, double disc grinder and polisher using emery papers of 120, 180, 320, 400, 600, 800 and 1000 grades. Buffing with alumina paste is done for mirror finishing to facilitate microstructure observation. Etching is done on the clad portion with copper-chloride ($CuCl_2$), diluted hydrochloric

Table 1 : Trial Run Data

Welding Voltage : 24 Volt (constant)									
So. No.	Weld Current (A)	Welding Speed (mm/s)	Heat Input (kJ/mm)	Continuity in deposition	Spatter	Reinforce-ment (R)	Bead width (W)	RFF	Remarks (Quality of weld bead)
1	100	11.6	0.166	Non-uniform	NIL	1.52	3.71	2.440	
2	130	11.6	0.215	Moderate	Very few	2.25	3.63	1.613	
3	100	8.7	0.221	Continuous	NIL	1.98	3.56	1.798	Acceptable
4	100	7.2	0.267	Continuous	NIL	1.79	5.66	3.162	Acceptable
5	125	8.7	0.276	Continuous	NIL	1.97	3.56	1.807	Acceptable
6	130	8.7	0.287	Continuous	Very few	1.68	3.85	2.292	
7	180	11.6	0.298	Discontinuous	NIL	2.54	3.27	1.287	
8	100	5.9	0.325	Continuous	NIL	1.92	6.35	3.307	Acceptable
9	150	8.7	0.331	Continuous	Moderate	2.14	4.84	2.262	Acceptable
10	125	7.2	0.333	Continuous	Few	1.96	5.80	2.959	Acceptable
11	150	7.2	0.400	Continuous	Few	2.46	5.44	2.211	
12	125	5.9	0.407	Continuous	NIL	2.97	5.58	1.879	Acceptable
13	150	5.9	0.488	Continuous	NIL	3.63	6.21	1.710	Acceptable
14	180	5.9	0.586	Continuous	Moderate	3.96	6.12	1.545	
15	200	5.9	0.651	Continuous	Too much	4.11	6.01	1.462	

Table 2 : Factors and their Levels

Parameter	Factor Levels		
	-1	0	+1
Welding current, I(A)	100	125	150
Welding Speed, S (mm/s)	5.9	7.2	8.7

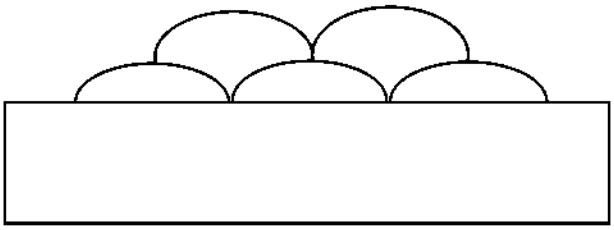

Fig. 1 Scheme of weld bead formation

acid (HCl, 40% v/v) and ethyl alcohol (C_2H_5OH, 99%) solution. The base plate is etched with nital (2% nitric acid with ethyl alcohol). Microstructure of the specimen is observed under an inverted metallurgical microscope (make: Metzar, India). Ferrite number (FN) is also calculated for the austenitic stainless steel using the standard relationship (equation 2) suggested by McGowan et al. (1986) [4] and it comes out to be 1.844.

$$FN = -15.2 + 2.2\,[Cr + Mo + 0.5\,Si + 15\,Ti + 0.8\,Nb] - 1.9\,[Ni + 17\,N + 30\,C] \quad (2)$$

Again, Chromium equivalent (Cr_{eq}) and Nickel equivalent (Ni_{eq}) are calculated using standard relationships as given in equation 3 and equation 4. Cr_{eq} and Nieq are found out to be 19.16 and 13.5 respectively. Corresponding ferrite content comes out to be around 2% from WRC 1992 diagram proposed by Welding Research Council [4]. This value is close to the ferrite number found out. This Cr_{eq} and Ni_{eq} point out that the austenitic stainless steel wire electrode is lying on AF zone where austenite content is predominant with only about 2% presence of ferrite.

Cr_{eq} = Cr + Mo +0.7 Nb (3)

Ni_{eq} = Ni + 35 C + 20 N + 0.25 Cu (4)

Corrosion test is carried out using a solution of ferric chloride ($FeCl_3$) with diluted HCl [0.05(N)] and ethyl alcohol (C_2H_5OH, 99%). Immersion corrosion test is conducted in the present work. Unclad region and some portions of clad surface are masked using Teflon. The exposed area of 20 x 12 sq. mm is maintained in all the specimens. Surface of the clad material is exposed to the corrosive solution and loss of weight of clad specimen is measured after dipping the exposed surface for 24 hours in the corroding medium and washing is thoroughly under running water. Weight of specimens before and after the corrosion test is measured on a digital weighing balance (resolution: 1 mg, range: 0-100 gm).

In this work, pitting index is also calculated for the base plate material and the wire electrode material using the following equation [4].

Pitting index = Cr + 3.3 Mo + 13 N (5)

3.0 RESULTS AND DISCUSSION ON TRIAL RUNS

Bead-on-plate experiments with 316 austenitic stainless steel electrodes are carried out in trial runs with varying combinations of welding current and welding speed on low alloy steel plates. By observing results of these trial runs, the working range of selected parameters is chosen. Results of trial runs in terms of continuity of weld deposition, spatter, and bead geometry are detailed in **Table 1.** Porosity and under-cutting are found absent in test runs. At 11.6 mm/s welding speed, lack of continuity of weld deposition is noted in all the experimental runs, and therefore, these experimental conditions are not chosen to carry out cladding experiments. Similarly, at a weld current of more than 150 A, that is, with higher heat input, weld bead formation is found not to be good and hence, not considered for cladding experiments.

It is seen that within welding speed of 5.9 mm/s to 8.7 mm/s, and 100A-150A of welding current, continuous deposition is observed with quite less, or no, spatter at all. Bead geometry parameters, such as, bead width (W) and reinforcement (R) are measured, and then reinforcement form factor (RFF= W/R) is calculated for clad specimens as shown in **Table 1.** Conditions showing acceptable beads can see from **Table 1.** Considering these results, working ranges of input variables are selected for conducting detailed experiments on cladding.

4.0 RESULTS AND DISCUSSION ON CLADDING EXPERIMENTS

A 2-factor 3-level full factorial experimental design is set for experimental investigation as shown in **Table 2.** With the selected welding current and welding speed, cladding experiments are carried out on the specified low alloy steel base plates. The observations of continuity of weld material deposition and spatter associated with cladding along with heat input are presented in **Table 3.**

Table 3 : Observation of Clad Specimens

Welding voltage: 24 volt					
Specimen No.	Welding speed, S (mm/s)	Current, I (A)	Heat input (kJ/mm)	Continuity in deposition	Spatter
1	5.9	100	0.325	√	No
2	5.9	125	0.407	√	No
3	5.9	150	0.488	√	Few
4	7.2	100	0.267	√	No
5	7.2	125	0.333	√	No
6	7.2	150	0.4	Discontinuous	Few
7	8.7	100	0.22	√	No
8	8.7	125	0.276	√	No
9	8.7	150	0.331	√	Few

From **Table 3**, it can be seen that few spatters are present at the experimental runs with welding current of 150A corresponding to higher heat inputs of a welding speed. At lower values of current, there is no spatter observed. This nature of spatter is quite common during metal active gas welding of steels using 100% CO_2 gas shield. For experimental run 6 done on specimen number 6 corresponding to 150A current and 7.2 mm/s welding speed with 0.4 kJ/mm heat input, acceptable continuity in weld deposition is not observed unlike rest of the eight specimens. For this reason, specimen number 6 is not considered for further testing.

4.1 Observation on Hardness

Hardness of the base plate before cladding is measured by a Rockwell Hardness Tester. Hardness of low alloy steel base plate is found to be 95 HRB in B-scale and 15 HRC in C-scale. After cladding, specimens are cut with a saw to a desired size, filed, belt ground and polished. Measured Rockwell hardness number for each experimental run is presented in **Table 4**. Only slight increase in hardness is obtained in the clad material in the order of 18-21 HRC. With the change in heat input in this work, no appreciable variation in hardness is noticed on the clad portion. As the cladding is made of austenitic stainless steel, some increase in hardness over that of low alloy steel base plate is expected naturally for the presence of a number of alloying elements in the cladding.

4.2. Observation of Microstructure

Fig. 2 typically indicates interface region of the base material and clad material under 100x magnification of specimen number 9. It shows good penetration of weld clad material into low alloy steel base material. This indicates good bonding of the clad layer. In all the clad samples, good amount of penetration of clad material into the base material is observed showing good bonding.

Fig. 3 through **Fig. 5** depict typically the microstructure of the weld-clad regions of some specimens. Predominant austenitic phase with grain boundary ferrite can be observed in all these microstructures. This supports on the whole the evaluated value of low ferrite number (1.844) and low ferrite content (2%) qualitatively. **Fig. 3, Fig. 4** and **Fig. 5** correspond to specimen numbers 2, 4 and 8 respectively. In specimen number 4 (**Fig. 4**), low heat input of 0.267 kJ/mm is applied and no directional solidification is observed at this position of specimen. **Fig. 5** shows microstructure on specimen No. 8 depicting directional solidification of austenite grains with ferrite boundary.

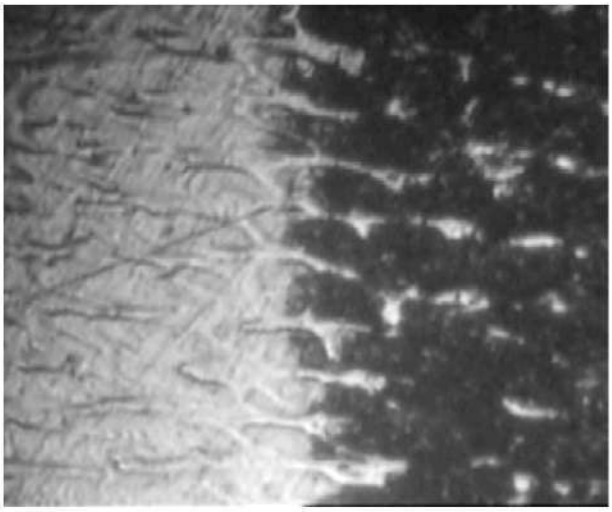

Fig. 2 : Weld interface of Specimen 9 [100x]

Table 4 : Hardness of the clad material observed

Specimen No.	Welding speed, S (mm/s)	Current, I (A)	Heat input (kJ/mm)	Mean hardness (HRC)
1	5.9	100	0.325	18
2	5.9	125	0.407	20
3	5.9	150	0.488	18
4	7.2	100	0.267	20
5	7.2	125	0.333	19
7	8.7	100	0.22	19
8	8.7	125	0.276	21
9	8.7	150	0.331	20

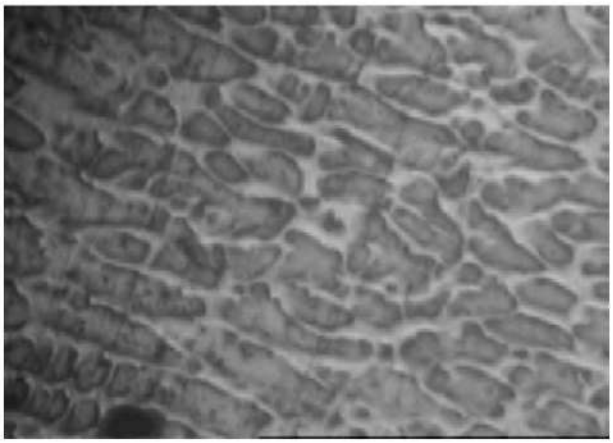

Fig. 3 : Microstructure of clad metal of Specimen 2 [20x]

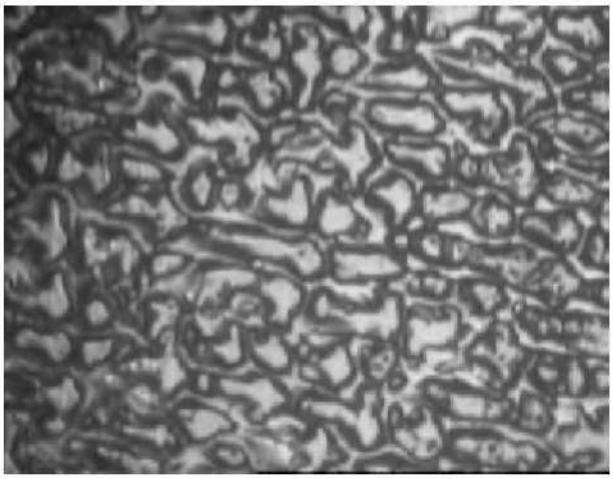

Fig. 4 : Microstructure of clad metal of Specimen 4 [20x]

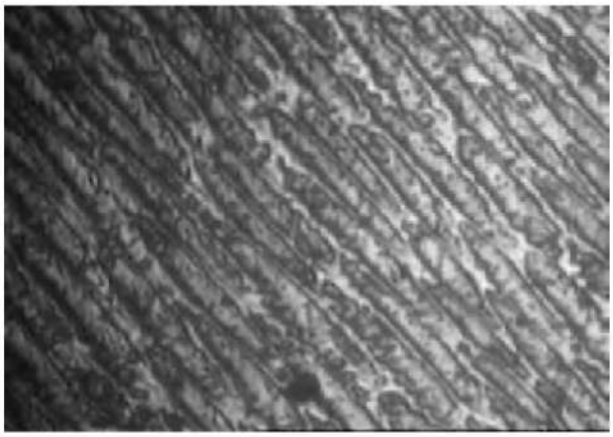

Fig. 5 : Microstructure of clad metal of Specimen 8 [20x]

4.3. Results of Corrosion Test

Corrosion tests on clad samples are conducted through immersion of Teflon masked specimens into the corrosive solution of ferric chloride ($FeCl_3$) with diluted HCl [0.05(N)] and ethyl alcohol (C_2H_5OH, 99%) for 24 hours. The exposed area of specimen is maintained to be 20 x 12 sq. mm. **Table 5** gives corrosion rates of austenitic stainless steel cladding of clad specimens as obtained from experimental results in an ascending order of heat input.

It can be stated that specimen number 7 corresponding to 100 A welding current and 8.7 mm/s speed of weld torch, and 0.22 kJ/mm heat input, gives the least corrosion rate of 34.44 gm/(m2.hr) of the tests made within the domain of this experimental work. On the other hand, clad specimen number 2 and 9 obtained using 125 A and 150 A current with 5.9 mm/s and 8.7 mm/s welding speed respectively under the

Table 5 : Results obtained from corrosion tests

Sl. No.	Specimen No.	Welding Speed S (mm/s)	Current, I (A)	Heat input (kJ/mm)	Corrosion rate (gm/[m^2,hr]}
1	7	8.7	100	0.22	34.44
2	4	7.2	100	0.267	37.34
3	8	8.7	125	0.276	39.09
4	1	5.9	100	0.325	39.58
5	9	8.7	150	0.331	41.47
6	5	7.2	125	0.333	40.86
7	2	5.9	125	0.407	41.49
8	3	5.9	150	0.488	39.19

corresponding heat input of 0.407 kJ/mm and 0.331 kJ/mm, show high corrosive wear rate of 41.49 and 41.47 gm/(m^2.hr). Therefore, 100 A welding current, 8.7 mm/s speed of weld torch with a constant 24 V weld voltage and giving 0.22 kJ/mm heat input, may be adopted for such applications that require less rate of corrosion. In fact, too high heat input may not yield good corrosion resistance as reported earlier also. Hence, it can be stated that moderate heat input of 0.22 kJ/mm may be recommended for adopting in relevant cladding work for raising service life of the base material of a component.

As the electrode has less ferrite number as well as ferrite content, expectedly, presence of ferrite phase is less, and this may have resulted in somewhat low resistance to corrosion compared to that using duplex stainless steel cladding as is reported in different works previously [4, 11, 17] on the whole.

Pitting index is calculated following equation 5. For low alloy steel, that does not contain molybdenum and nitrogen, has the pitting index of 2.02 whereas 316 austenitic stainless steel shows a high pitting index of 23.76. Molybdenum content of 2% and chromium content of 17.16% is the main reason behind this large pitting index of 316 steel indicating the feasibility of having superior corrosion resistance of it as the clad layer over the corrosion prone low alloy steel base plate. Results also validate this proposition showing fairly good corrosion resistance of the 316 stainless steel cladding over that observed in low alloy steel base plate as reported by Verma et al. [11, 12, 17].

5.0 CONCLUSIONS

Following conclusions may be drawn from the observations on cladding of low alloy steel base plates with 316 austenitic stainless steel electrode using GMAW process under CO_2 gas shield;

- Except experiment number 6, good reinforcement with lesser penetration is noticed in all the cladding experiments indicating applicability of this cladding technique.
- Hardness of clad layer has increased slightly over that of base material having hardness of 15 HRC and is found to be within 18 to 21 HRC without much variation with the increase in heat input.
- Microstructural observation indicates presence of austenitic grain structure with ferrite grain boundary. Interface of base material with cladding indicates good bonding between them. Less ferrite content as well as ferrite number is found out in the clad region indicating low share of ferrites and hence, somewhat less corrosion resistance in this work compared to duplex stainless steel.
- Relatively less rate of corrosion is obtained at 100A welding current, 8.7 mm/s welding torch travel speed, 24V welding voltage with 0.22 kJ/mm heat input after 24 hours of immersion type corrosion test compared to all other conditions tested. Hence, this condition may be adopted for cladding on low alloy steel components.

REFERENCES

[1] P. K. Palani and N. Murugan, Development of mathematical models for prediction of weld bead geometry in cladding by flux cored arc welding, Int. J Adv Manuf. Tech., vol.30, pp.669–676, 2006.

[2] P. K. Palani and N. Murugan, Optimisation of weld bead geometry for stainless steel cladding deposited by FCAW, J Mat. Proc. Tech., vol.190, pp.291-299, 2007.

[3] T. Kannan and J. Yoganandh, Effect of process parameters on clad bead geometry and its shape relationships of stainless steel claddings deposited by GMAW, Int. J Adv Manuf. Tech., vol.47, pp.1083–1095, 2010.

[4] B. Chakrabarti, H. Das, S. Das and T. K. Pal, Effect of process parameters on clad quality of duplex stainless steel using GMAW process, Trans. Indian Inst. of Metals, Vol.66, No.3, pp.221-230, 2013.

[5] T. Kannan and N. Murugan, Effect of flux cored arc welding process parameters on duplex stainless steel clad quality, J Mat. Proc. Tech., vol.176, pp.230-239, 2006.

[6] A. S. Shahi and S. Pandey, Modeling of the effects of welding conditions on dilution of stainless steel cladding produced by GMAW, J Mat. Proc. Tech., vol.196, pp.339-344, 2008.

[7] N. Alam, J. Wu and T. Kilpatrick, Laser and PTA deposited alloys for erosion resistance applications, Proc. IIW Int Conf. on Global Trends in Joining, Cutting and Surfacing Tech., Chennai, pp.351-357, 2011.

[8] R. Pull, E. N. Kumar and G. D. J. Ram, Studies on austenitic stainless steel AISI 316L friction surfaced coatings, Proc. IIW Int. Conf. on Global Trends in Joining, Cutting and Surfacing Tech., Chennai, pp.111-116, 2011.

[9] A. K. Singh and G. M. Reddy, Effect of process parameters on bead strength of stainless steel metal coating of low alloy steel by surfacing route, Proc. IIW Int. Conf. on Global Trends in Joining, Cutting and Surfacing Tech., Chennai, pp.125-130, 2011.

[10] N. V. Rao, G. M. Reddy and S. Nagarjuna, Weld overlay cladding of high strength low alloy steel with austenitic stainless steel– structure and properties, Mat. and Des., Vol. 32, pp. 2496-2506, 2011.

[11] A. K. Verma, B. C. Biswas, P. Roy, S. De, S. Saren and S. Das, Exploring quality of austenitic stainless steel clad layer obtained by metal active gas welding, Indian Sc. Cruiser, Vol.27, No.4, pp.24-29, 2013.

[12] A. K. Verma, B. C. Biswas, P. Roy, S. De, S. Saren and S. Das, On the performance of cladding austenitic stainless steel on plain carbon steel, Proceedings of the Seminar on Welding Management for Sustainable Development, Visakhapatnam, India, pp.1-9, 2013.

[13] J. Adamiec, High temperature corrosion of power boiler components cladded with nickel alloys, Mat. Charact., vol.60, pp.1093-1099, 2009.

[14] V. Kumar, G. Singh and M. Z. Khan Yusufzai, Effects of Process Parameters of Gas Metal Arc Welding on Dilution in Cladding of Stainless Steel on Mild Steel, MIT Int. J of Mech. Engg, Vol.2, No.2, pp.127-131, 2012.

[15] P. K. Ghosh, P. C. Gupta and V. K. Goyal, Stainless Steel Cladding of Structural Steel Plates Using The Pulsed Current GMAW Process, Welding Res. Supple., Welding J, pp.307s-314s, 1998.

[16] M. Nouri, A. Abdollah-Zadeh and F. Malek, Effect of Welding Parameters on Dilution and Weld Bead Geometry in Cladding, J of Mat. Sc. and Tech., Vol.23, No.6, pp.817-822, 2007.

[17] A. K. Verma, B. C. Biswas, P. Roy, S. De, S. Saren and S. Das, On the effectiveness of duplex stainless steel cladding deposited by gas metal arc welding, eProc. of the Int. Conf. of the Int. Inst. of Welding, Seoul, Korea, 2014.

[18] ASTM-G-31-72, Standard Practice for Laboratory Immersion Corrosion Testing for Metals, ASTM, 1998.

[19] R. A. Perren, T. A. Suter, P. J. Uggowitzer, L. Weber, R. Magdowski, H. Bohni and M. O. Speidel, Corrosion resistance of super duplex stainless steels in chloride ion containing environments: investigations by means of a new microelectro chemical method, 1. precipitation–free states, Corrosion Sc., vol.43, pp.707-726, 2001.

[20] W. T. Tsai and J. R. Chen, Galvanic corrosion between the constituent phases in duplex stainless steel, Corrosion Sc., vol.49, pp.3659-3668, 2007.

[21] K. Sabiruddin, S. Das and A. Bhattacharya, Application of the analytic hierarchy process for optimization of process parameters in GMAW, Ind. Welding J, vol.42, No.1, pp.38-46, 2009.

[22] A. Sarkar and S. Das, Application of grey-based Taguchi method for optimizing gas metal arc welding of stainless steels, Ind. Welding J, vol.44, No.1, pp.37-48, 2011.

[23] D. S. Correia, C. V. Goncalves, S. C. J. Sebastiao and V. A. Ferraresi, GMAW welding optimization using genetic algorithms, J. Brazilian Soc. of Mech. Sc. and Engg., Vol.XXVI, No.1, pp.28-33, 2004.

[24] E. Karadeniz, U. Ozsarac and C. Yildiz, The effect of process parameters on penetration in gas metal arc welding process, Mat. and Des., vol.28, pp.649-656, 2007.

[25] K. Sabiruddin, S. Bhattacharya and S. Das, Selection of appropriate process parameters for gas metal arc welding of medium carbon steel specimens, Int. J of Analytical Hierarchy Process, Vol.5, No.2, pp.252-267, 2013.

[26] H. Sieurin and R. Sandström, Sigma Phase Precipitation in Duplex Stainless Steel 2205, Mat. Sc. and Engg A, pp.271-276, 2007.

[27] Y. Pan and C. Qiu, Phase Diagrams and σ-Phase Precipitation in Some Stainless Steels, Trans. of the National Foundry Society, Vol. 5, No.2, pp.76-84, 1995.

[28] T. Huhtala, J. O. Nilsson, P. Jonsson and A. Wilson, Influence of W and Cu on Structural Stability of Super Duplex Weld Metals, Proceedings of 4th Int. Conf. on Duplex Stainless Steels, Glasgow, Scotland, Paper 43, pp.13-16, 1994.